CardioVascular and Interventional Radiology

Cardiovasc Intervent Radiol (1999) 22:321–325

LABORATORY INVESTIGATION

Pulmonary Hemorrhage: Imaging with a New Magnetic Resonance Blood Pool Agent in Conjunction with Breathheld Three-Dimensional Magnetic Resonance Angiography

Dominik Weishaupt, Paul R. Hilfiker, Michaela Schmidt, Jörg F. Debatin

Institute of Diagnostic Radiology, University Hospital Zurich, Rämistrasse 100, CH-8091 Zurich, Switzerland

Abstract

Purpose: To describe the three-dimensional magnetic resonance angiography (3D MRA) imaging appearance of the pulmonary arteries following administration of a superparamagnetic iron oxide blood pool agent to human volunteers, and to demonstrate in an animal model (pigs) how this technique can be used to detect pulmonary parenchymal hemorrhage.

Methods: Two volunteers were examined following the intravenous administration of a superparamagnetic iron oxide blood pool agent (NC100150 Injection, Nycomed Amersham Imaging, Wayne, PA, USA). T1-weighted 3D gradient recalled echo (GRE) image sets (TR/TE 5.1/1.4 msec, flip angle 30°) were acquired breathheld over 24 sec. To assess the detectability of pulmonary bleeding with intravascular MR contrast, pulmonary parenchymal injuries were created in two animals under general anesthesia, and fast T1-weighted 3D GRE image sets collected before and after the injury.

Results: Administration of the intravascular contrast in the two volunteers resulted in selective enhancement of the pulmonary vasculature permitting complete visualization and excellent delineation of central, segmental, and subsegmental arteries. Following iatrogenic injury in the two animals, pulmonary hemorrhage was readily detected on the 3D image sets.

Conclusion: The data presented illustrate that ultrafast 3D GRE MR imaging in conjunction with an intravenously administered intravascular blood pool agent can be used to perform high-quality pulmonary MRA as well as to detect pulmonary hemorrhage.

Key words: Contrast media—Pulmonary angiography—Pulmonary hemorrhage—MR angiography

Correspondence to: J.F. Debatin, M.D.

The imaging performance of fast three-dimensional MR angiography (3D MRA) with regard to the pulmonary arteries may be enhanced by the use of intravascular MR contrast agents [1]. Since the long intravascular half-life of intravascular MR contrast agents no longer limits data collection, the pulmonary vasculature can be imaged repeatedly [1]. Moreover, any disruption of pulmonary arterial vascular integrity should result in extravasation and accumulation of the intravascular agent within the pulmonary parenchyma, permitting easy detection and localization of hemorrhagic sites.

The availability of high-performance gradient systems has shortened imaging times sufficiently to permit collection of a complex 3D gradient recalled echo (GRE) data set within the confines of a convenient breathhold [2]. In conjunction with the well-timed administration of an intravenous bolus of extracellular, T1-shortening paramagnetic contrast agents, the entire pulmonary arterial vasculature can be imaged with sufficient spatial resolution to resolve even sixth-generation vessels [3].

Pulmonary hemorrhage can be either localized or diffuse [4]. Diffuse pulmonary hemorrhage is rare. Caused by an immune or coagulation disorder, it can lead to hemoptysis and iron deficiency anemia [5]. Localized pulmonary hemorrhage, on the other hand, is considerably more common and usually secondary to chronic bronchitis, bronchiectasis, tumors, or localized infections. Delivery of potentially life-saving surgical, endobronchial, or endovascular therapy is predicated upon the quick and accurate localization of the bleeding site. The value of plain chest radiography, high-resolution CT, and fiberoptic bronchoscopy in this regard is firmly established. Despite the use of these modalities, localization of bleeding sites can remain difficult or even impossible [6, 7].

This study addresses the value of 3D MR imaging following the intravenous administration of an intravascular superparamagnetic iron oxide blood pool agent. The under-

lying imaging technique for visualization of the pulmonary vasculature using maximum intensity projections (MIPs) is illustrated. In addition, the use of this technique for detecting pulmonary parenchymal bleeding is demonstrated in pigs.

Materials and Methods

Intravascular Contrast Agent

NC100150 Injection (Nycomed Amersham Imaging, Wayne, PA, USA) is a new MR blood pool contrast agent. It is a colloidal preparation of ultrasmall superparamagnetic iron oxide crystals with an oxidized starch coating. One milliliter of NC100150 Injection contains 30 mg of iron (Fe). The total particle diameter (iron oxide core with coating) is less than 25 nm. Superparamagnetic iron oxide contrast agents are endocytosed and metabolized by cells of the reticuloendothelial system (RES), primarily by the Kupffer cells in the liver. The iron is incorporated into the normal metabolic iron pool in the same way as iron is absorbed from the diet. This agent has been shown to be safe in phase I trials on human volunteers, when administered intravenously as a bolus in doses up to 4 mg/kg body weight [8]. The vascular half-life in humans is dose-dependent and ranges from 3 to 4 hr [8]. NC100150 causes considerable shortening of both T1 and T2 relaxation times. On heavily T1-weighted fast 3D GRE acquisitions, characterized by short repetition (TR) and echo (TE) times, the T1-shortening effects predominate [8].

MR Imaging

All MR imaging was performed on a 1.5-Tesla (T) MR system (Signa EchoSpeed; GE Medical Systems, Milwaukee, WI, USA) equipped with an ultrafast three-axis gradient system characterized by an amplitude of 22 mT/m and a slew rate of 140 mT/m/msec. An anteroposterior phased-array surface coil (torso array coil) was used for signal reception. Patients were imaged in the supine position with their arms above their head to prevent aliasing. 3D MRA data were acquired using a 3D Fourier transform GRE sequence with spoiling gradients in the coronal plane [2]. TR and TE were 5.1 and 1.4 msec, respectively. The flip angle was 30°. The sampling bandwidth was ± 62.5 kHz. A 40 × 40 cm FOV coupled with a 256 × 192 matrix rendered an in-plane resolution of 1.5 mm × 2.1 mm. Partial (0.6) *k*-space sampling in the phase-encoding direction permitted the breathheld acquisition of 48 contiguous coronal sections in 24 sec. A section thickness of 2.0 mm covered an anteroposterior volume of 96 mm.

The imaging data were postprocessed into MIPs as well as 2-mm-thick 3D multiplanar reformations in the axial and coronal planes.

Human Imaging

Two healthy male volunteers (22 and 24 years old) underwent MR imaging of the chest following the intravenous administration of NC100150. The contrast material was administered by hand at a rate of approximately 3 ml/sec via a 20 gauge needle placed in the antecubital vein. The first subject received a dose of 3 mg Fe/kg body weight (6.5 ml) and the second subject a dose of 4 mg Fe/kg body weight (10.6 ml). The study had been approved by the Institutional Review Board of our hospital, and written informed consent was obtained from both subjects prior to beginning the study. Various safety parameters including blood pressure, heart rate, and body temperature were monitored continuously over the first 30 min following injection and subsequently at set intervals. A 12-lead electrocardiogram was acquired at 1, 2, 24, 48, and 72 hr following injection. Fluids for laboratory parameters (serum chemistry, hematology, and urinalysis) were collected at 10 min and 2, 24, 48, and 72 hr following injection. All data were compared with baseline values determined 24 hr and 30 min prior to injection.

Qualitative assessment of the MR images was based on visual interpretation of image quality. Signal intensity measurements were performed in a region of interest (ROI) placed within the pulmonary outflow tract, both central arteries, and all five lobar arteries, as well as in one segmental and one subsegmental artery of each lobe. Based on these 18 different measurements per 3D data set, the contrast-to-noise ratio (CNR) was calculated by dividing the absolute difference between the intravascular signal intensities and those determined in adjacent lung parenchyma by the standard deviation of the background image intensity [9].

Animal Experiments

Two female pigs weighing 35 and 41 kg were studied. The experiments were approved by the local animal use committee and conducted in accordance with all state regulations governing animal experiments. All procedures were performed under general anesthesia induced intravenously with ketamine-HCl 150 mg/10 kg body weight (Ketasol, Dr E. Gräub, Berne, Switzerland) and azaperone 10 mg/10 kg body weight (Stresnil, Veterinaraia, Zurich, Switzerland). Both animals were intubated and fully relaxed with pancuronium bromide 84 mg/2 hr (Pavulon, Organon, Teknika, Pfaeffikon, Switzerland). The anesthetic effect was maintained throughout the experiments by ventilating the animals with halothane 1.5% (Synmedic, Zurich, Switzerland).

Following the intravenous bolus administration of NC100150 in a dose of 4.0 mg Fe/kg body weight, the animals were imaged in the supine position. Based on 2D GRE localizing images, a 3D GRE data set was acquired of the pulmonary arteries in the coronal plane, using the parameters outlined above. Subsequently, a parenchymal lesion was created percutaneously with a 14 gauge needle in the lower lobe of the left lung. The needle path was monitored on fast 2D GRE images. Subsequent 3D GRE data sets were collected at 4-min intervals for 20 min.

Following completion of the experiment, the animals were killed by intravenous injection of potassium chloride. The lung was inspected for the presence of blood and confirmation of the localization of the parenchymal hemorrhage.

Analysis of the imaging data acquired during the animal experiments was based on individual sections, MIPs, and 2-mm-thick multiplanar reformations in the axial and sagittal planes.

Results

Human Volunteers

The intravenous administration of NC100150 was well tolerated by both subjects. There were no serious adverse events. No clinically significant changes were recorded. Laboratory analysis revealed an expected increase in serum iron.

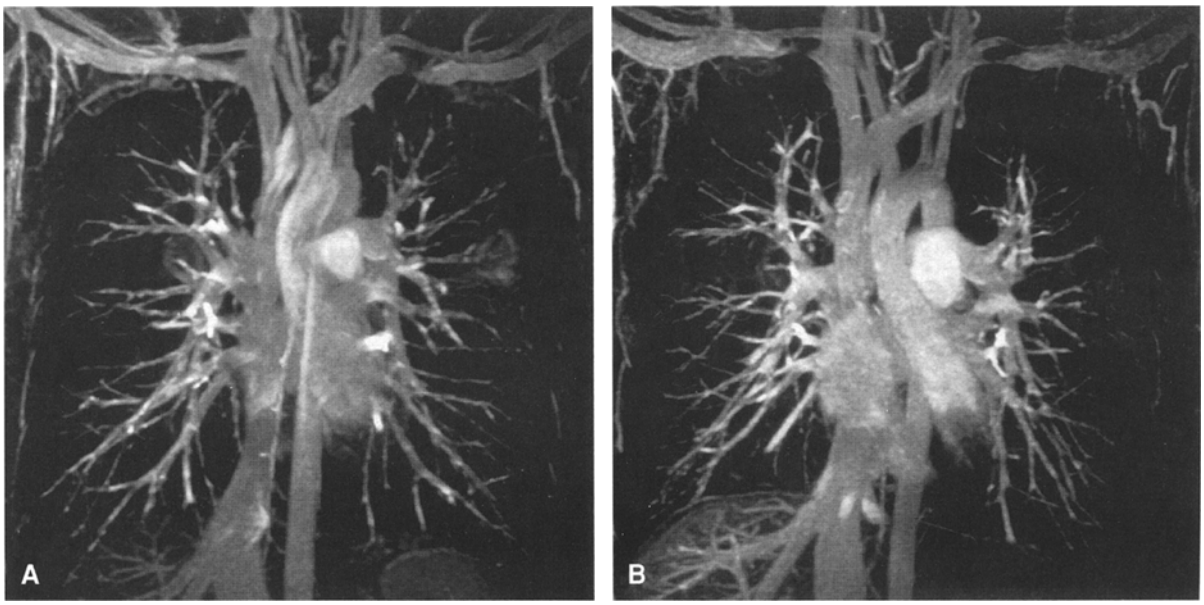

Fig. 1. Maximum intensity projection (MIP) reconstructions of 3D magnetic resonance angiography (MRA) data sets collected after the intravenous administration of NC100150 in normal volunteers. With both dosages (**A**, 3 mg Fe/kg body weight; **B** 4 mg Fe/kg body weight) the pulmonary arteries are visualized to the subsegmental level. Note the presence of overlapping veins.

Table 1. Contrast-to-noise ratios (CNR) of the pulmonary outflow tract, main stem, lobar, and segmental arteries

	3 mg Fe/kg body weight	4 mg Fe/kg body weight
Outflow tract	32	32
Main stem artery	26 ± 2	22 ± 2
Lobar arteries	22 ± 5	28 ± 2
Segmental arteries	19 ± 8	22 ± 5
Subsegmental arteries	11 ± 3	15 ± 3

High-quality MR angiograms were obtained with both doses (Fig. 1). The pulmonary arteries were depicted to the level of sub-subsegmental arteries. Pulmonary veins enhanced to the same degree as pulmonary arteries. Venous overlap obscured assessment of the arterial morphology on MIP images. Arteriovenous differentiation was easily accomplished, however, based on the coronal images, axial, and sagittal reformations.

The qualitative assessment is mirrored by the quantitative analysis (Table 1). CNR values were dependent on dose as well as on vessel size and location. They ranged from 26 to 28 in the outflow tracts, from 19 to 22 in the segmental pulmonary arteries, and from 11 to 15 in subsegmental pulmonary arteries. Mean CNR averaged over all 18 measurement locations was 19 ± 8 for the 3 mg Fe/kg body weight dose and 23 ± 7 for the 4 mg Fe/kg body weight dose. A paired Student's t-test revealed the differences between the two measurement sets to be statistically significant ($p < 0.05$).

Animal Experiments

The animals remained hemodynamically stable throughout the experiments. 3D data sets collected following the intravenous administration of NC100150 depicted the pulmonary arteries as homogeneously bright structures to their subsegmental level. The bleeding sites within the left lower lobes were identified as enlarging areas of bright signal on the 3D data sets. Over time the contrast spread within the pulmonary parenchyma became clearly visible (Fig. 2). The relationship between the bright pulmonary vasculature and the bleeding site was well delineated. Reflecting the percutaneous nature of the injury, contrast accumulation was observed in the pleural space over time. In both animals, autopsy findings confirmed the location of the pulmonary lacerations in the lower lobe of the left lung.

Discussion

Administration of NC100150 Injection caused no adverse effects in the two human subjects. In conjunction with fast T1-weighted 3D GRE sequences, the intravascular agent provided complete visualization of the pulmonary arterial tree to a subsegmental level. Beyond considerably widening the imaging window for repeated and possibly even high-resolution 3D MRA of the pulmonary arteries, the agent appears well suited for the quick detection and accurate localization of pulmonary hemorrhage sites.

Fast data acquisition strategies, based upon the availability of high-performance gradient systems, have laid the foundation for breathheld pulmonary MR imaging. T1-

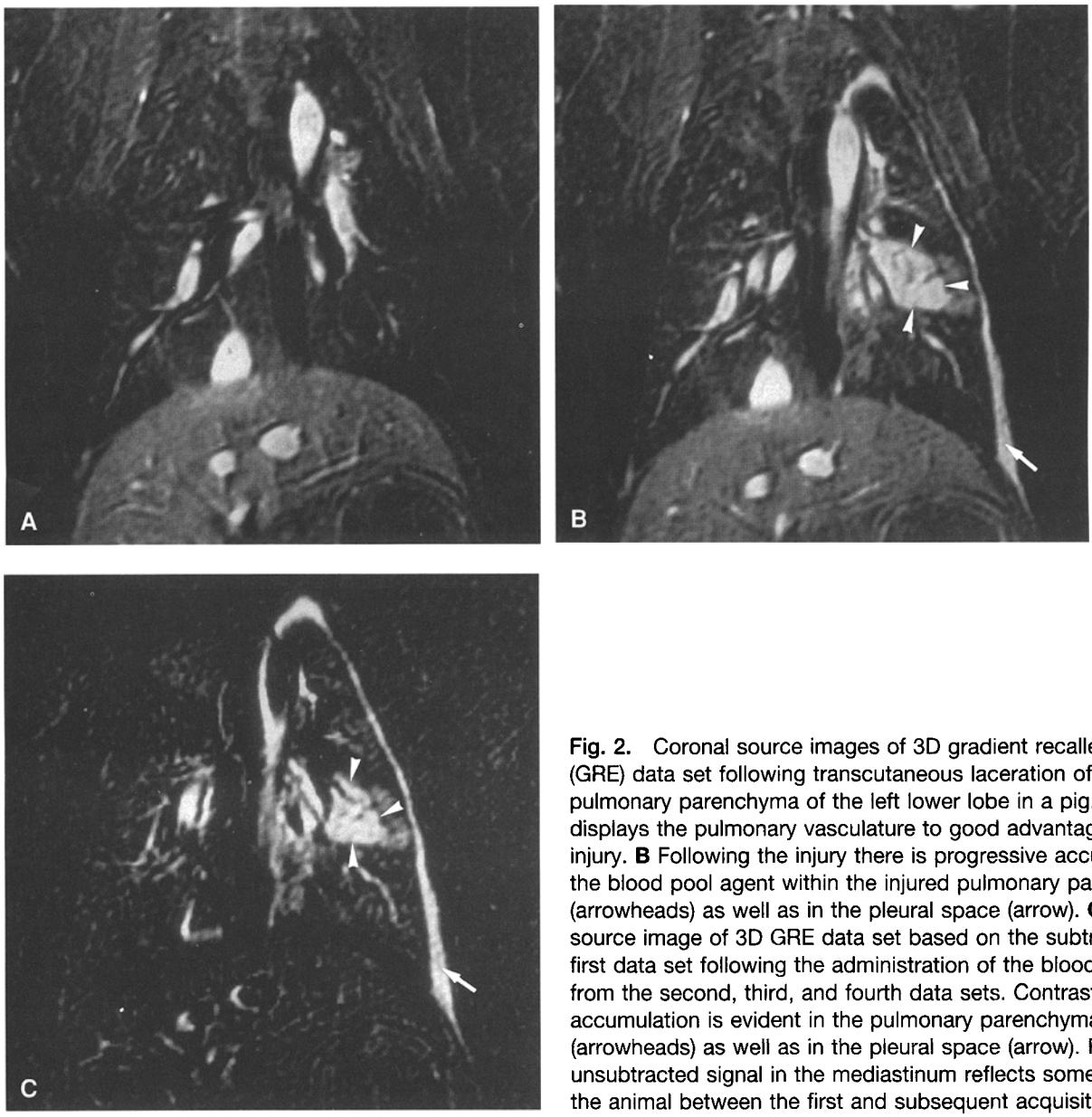

Fig. 2. Coronal source images of 3D gradient recalled echo (GRE) data set following transcutaneous laceration of the pulmonary parenchyma of the left lower lobe in a pig. **A** 3D MRA displays the pulmonary vasculature to good advantage before the injury. **B** Following the injury there is progressive accumulation of the blood pool agent within the injured pulmonary parenchyma (arrowheads) as well as in the pleural space (arrow). **C** Coronal source image of 3D GRE data set based on the subtraction of the first data set following the administration of the blood pool agent from the second, third, and fourth data sets. Contrast accumulation is evident in the pulmonary parenchyma (arrowheads) as well as in the pleural space (arrow). Residual unsubtracted signal in the mediastinum reflects some motion of the animal between the first and subsequent acquisitions.

weighted 3D GRE data sets with spatial resolution sufficient to delineate even small structures such as subsegmental pulmonary arteries can be acquired in under 20 sec [3]. Further improvements in gradient technology promise to reduce the underlying repetition and echo times even further in the near future, thereby further shortening the required breathhold intervals [10].

For 3D MRA, fast 3D GRE acquisitions are timed to coincide with the intravascular phase of intravenously administered T1-shortening extracellular paramagnetic contrast agents [11]. Hence, the technique provides homogeneous intravascular signal independent of flow effects and related artifacts. Recent years have seen the rapid implementation of contrast-enhanced 3D MRA for the assessment of virtually all vascular territories. Thus 3D MRA has been shown to be accurate in the assessment of the thoracic and abdominal aorta, the renal and mesenteric arteries, as well as the pelvic arterial system [12–15]. Similarly, the pulmonary arterial tree can be depicted to good advantage [2]. Recently Meaney et al. [16] reported contrast-enhanced 3D MRA to be highly accurate in the diagnosis of pulmonary embolism.

To date gadolinium chelates have been used as contrast media for 3D MRA. The agents are limited by their extracellular nature, resulting in a short intravascular half-life due to rapid redistribution into the extracellular spaces. Background noise induced by the extracellular redistribution and dosing limitations virtually prohibit repeated image acquisitions of the same region in the case of technical failure or its extension to a second vascular territory. Breathheld contrast-enhanced 3D pulmonary MR imaging using gadolinium has been associated with a high sensitivity and specificity for the diagnosis of pulmonary embolism [15]. However, most patients with sus-

pected pulmonary embolism are severely dyspneic and do not tolerate breathheld data acquisition of large vascular territories. Intravascular contrast agents, by providing a long imaging window, promise to overcome these limitations [1].

NC100150 is a colloidal presentation of coated ultrasmall superparamagnetic iron oxide particles, capable of inducing vast reductions in both T1 and T2 relaxation times (internal study reports, Nycomed Amersham Imaging). Employed in combination with an ultrafast 3D GRE acquisition characterized by short repetition and echo times, the T1-shortening effects predominate, rendering the intravascular signal exquisitely bright. CNR levels within the subsegmental pulmonary arteries exceeding a value of 10 illustrate this phenomenon to good advantage. Although the CNR values were somewhat dose-dependent, favoring the higher 4 mg Fe/kg body weight dose, the pulmonary vasculature was sufficiently well delineated even with a dose of 3 mg Fe/kg body weight. In view of the slightly better results, the 4 mg/kg dose was used for the animal experiments.

High-quality arterial-phase images can be obtained with intravascular contrast agents by imaging dynamically during the arterial phase of the injection, as is currently practiced with extracellular gadolinium contrast agents. In addition, intravascular agents permit continued imaging in the equilibrium "intravascular" phase. This allows for repetitive imaging of focused regions and may thus prove particularly helpful in the diagnostic investigation of patients with suspected pulmonary emboli. The image quality achieved in this limited study of two volunteers illustrates excellent depiction of the entire pulmonary arterial tree.

Furthermore, the intravascular nature of the agent results in extravasation of contrast only in areas of compromised vascular integrity: areas of active bleeding are thus readily detected and accurately located. This rather simplistic observation promises to influence considerably the list of potential indications for NC100150 Injection, as well as any other intravascular contrast agent. Although very preliminary and somewhat crude, the animal experiments described here do document the feasibility of intravascular MR contrast agents in conjunction with fast 3D GRE acquisitions to locate the origin of pulmonary parenchymal hemorrhage. The long intravascular half-life of the agent permits repetitive imaging over a longer time frame during which the agent has accumulated in the extravascular space, thereby enhancing conspicuity. In this respect, the proposed technique mimics radionuclide studies. At the same time, the high-resolution 3D data sets provide a detailed depiction of the surrounding vascular and parenchymal morphology similar to conventional angiography.

Bleeding from the lung is most frequently caused by a local injury to the vascular bed induced by processes such as chronic bronchitis, bronchiectasis, tumors, or localized infections. The diagnostic investigation of pulmonary bleeding remains controversial [6, 7]. The combined use of fiberoptic bronchoscopy and CT has to date yielded the best results in the investigation of patients with hemoptysis [6]. Despite best efforts, pulmonary bleeding sites often remain unidentified, even in patients with moderate to severe hemoptysis [6, 7]. Fast 3D GRE imaging in the presence of intravascular blood pool agents promises to solve this diagnostic dilemma. In addition, the technique may prove useful in the characterization of diffuse pulmonary diseases, based upon their effect on the integrity of the vascular bed. Thus it is conceivable that this technique may permit an earlier or more specific diagnosis of angiocentric disease processes, such as invasive aspergillosis, known to cause micro-infarctions with localized pulmonary hemorrhage.

In summary, the data presented here illustrate that ultrafast 3D GRE MR imaging in conjunction with an intravenously administered intravascular blood pool agent can be used to perform high-quality pulmonary MRA as well as to detect pulmonary hemorrhage.

References

1. Anzai Y, Prince MR, Chenevert TL, Maki JH, Londy F, London M, McLachlan SJ (1997) MR angiography with superparamagnetic iron oxide blood pool agent. J Magn Reson Imaging 7:209–214
2. Leung DA, McKinnon GC, Davis CP, Pfammatter T, Krestin GP, Debatin JF (1996) Breath-hold contrast-enhanced, three-dimensional MR angiography. Radiology 201:569–571
3. Steiner P, McKinnon GC, Romanowski B, Goehde SC, Hany T, Debatin JF (1997) Contrast-enhanced, ultrafast 3D MR angiography in a single breath-hold: Initial assessement of imaging performance. J Magn Reson Imaging 7:177–182
4. Frazer RG, Paré P, Paré PD (1988) Diseases of the thorax caused by eternal physical agents. In: Fraser RG, Paré P, Paré PD (eds) Diagnosis of Diseases of the Chest, 3rd edn. WB Saunders, Philadelphia. pp 394–396
5. Primack SL, Miller RR, Müller NL (1995) Diffuse pulmonary hemorrhage: Clinical, and imaging features. AJR 164:295–300
6. Hirschberg B, Biran I, Glazer M, Kramer MR (1997) Hemoptysis: Etiology, evaluation and outcome in a tertiary referral hospital. Chest 112:440–444
7. McGuinness G, Beacher JR, Harkin TJ, Garay SM, Rom WN, Naidich DP (1994) Hemoptysis: Prospective high-resolution CT/bronchoscopic correlation. Chest 105:1155–1162
8. Wildermuth S, Dubno B, Romanowski J, Borseth A, Annweiler A, Debatin JF (1998) Open-label, phase 1 trial of a new blood pool contrast agent (NC100150) in 12 healthy volunteers: Safety and vascular imaging characteristics. Sixth Annual Scientific Meeting of the International Society of Magnetic Resonance in Medicine (ISMRM), Sidney, 1998
9. Shott S (1990) Nonparametric statistics. In: Statistics for Health Professionals. WB Saunders, Philadelphia. pp 229–267
10. Heid O, Deimling M, Huk WJ (1995) Ultra-rapid gradient echo imaging. J Magn Reson Imaging 33:143–149
11. Prince MR (1994) Gadolinium-enhanced MR aortography. Radiology 191:155–164
12. Prince MR, Yucel EK, Kaufman JA, Harrison DC, Geller SC (1993) Dynamic gadolinium-enhanced three-dimensional abdominal MR arthrography. J Magn Reson Imaging 3:877–881
13. Holland GA, Dougherty L, Carpenter JP, Axel L (1996) Breath-hold ultrafast three-dimensional gadolinium-enhanced MR angiography of the aorta and the renal and other visceral arteries. AJR 166:971–981
14. Snidow JJ, Johnson MS, Harris VJ, Margosian PM, Aisen AM, Lalka SG, Cikrit DF, Trerotola SO (1996) Three-dimensional gadolinium-enhanced MR angiography of aortoiliac inflow assessment plus renal artery screening in a single breath hold. Radiology 198:725–732
15. Hany TF, Debatin JF, Leung DA, Pfammatter T (1997) Evaluation of aortoiliac and renal arteries: Comparison of breath-hold, contrast-enhanced, three-dimensional MR angiography with conventional catheter angiography. Radiology 204:357–362
16. Meaney JF, Weg JG, Chenevert TL, Stafford-Johnson D, Hamilton BH, Prince MR (1997) Diagnosis of pulmonary embolism with magnetic resonance angiography. N Engl J Med 336:1422–1427